Synthesis and optical properties of $PbMoO_4$ nanoplates

Runping Jia (贾润萍)* and Yingqiang Zhang (张英强)

School of Materials Science and Engineering, Shanghai Institute of Technology, Shanghai 200235, China

**E-mail: jiarp@sit.edu.cn*

Received June 22, 2010

Nanometer sized lead molybdate ($PbMoO_4$) plates are prepared through conventional hydrothermal together with sonochemical methods. The plates are then characterized using field-emission scanning electron microscopy, X-ray diffractometry, Fourier transform infrared (FTIR) spectrometry, photoluminescence spectrometry, and ultraviolet-visible (UV-VIS) spectrometry. The results indicate that the nanoplates have a characteristically narrow particle size distribution and their tetragonal scheelite-type structure is confirmed by both X-ray diffractometry and FTIR spectrometry. When the nanoplates are compared with the corresponding bulk crystals, blue shifts in their photoluminescence peaks, wider optical band gaps, and the broadening of the X-ray diffractometer peaks are observed. These can be ascribed to the decrease in crystal size.

OCIS codes: 160.2540, 160.4236, 160.4670.

doi: 10.3788/COL20100812.1152.

The characteristics of many modern materials are often determined by the properties of their nanoparticles, especially their shapes and sizes. This fact is responsible for the fast-growing demand for the analysis of nanoparticle size and shape to meet with a variety of applications[1,2]. Given that tetragonal scheelite-type molybdates and tungstates have divalent cationic radii larger than 0.099 nm, such as Ca^{2+}, Sr^{2+}, Ba^{2+}, and Pb^{2+}, as well as molybdenum (Mo^{6+}) and tungsten (W^{6+}) ions, such materials present tetrahedral coordination[3−5]. They have recently attracted particular interest in a variety of applications, such as laser host materials, luminescent materials, microwave applications, scintillators, and so on[6−8]. Among the said materials, lead molybdate ($PbMoO_4$) is the most promising candidate as a scintillator for double β decay experiments at temperatures below 100 K[9]. Various methods, such as wet chemical processes, microwave radiation, and microwave-hydrothermal, have been used to synthesize molybdates and tungstates up until now[10−13]. However, the particles of molybdates and tungstates prepared using the aforementioned processes are relatively large and have an irregular morphology[14,15].

Therefore, novel-shaped $PbMoO_4$ nanoplates were prepared through the combination of conventional hydrothermal and sonochemical methods. The crystalline phase, particle morphology, particle size distribution, and optical properties were investigated through X-ray diffraction (XRD) patterns, field-emission scanning electron microscopy (FESEM), Fourier transform infrared (FTIR) spectroscopy, ultraviolet–visible (UV–VIS) absorption spectroscopy, and photoluminescence (PL) measurements. The advantage of using these methods is that they are simple, fast, efficient, economical to process, environment-friendly, and viable for large-scale production. This will offer more application opportunities in the field of luminescence.

The $PbMoO_4$ nanoplates were synthesized through conventional hydrothermal and sonochemical methods. The experimental procedure is described in detail in the following discussions. A fixed volume and concentration of lead chloride ($PbCl_2$) (98% purity, Sigma-Aldrich) solution was added into a 50-mL glass beaker and ultrasonicated at a frequency of 40 kHz. Afterwards, equimolar sodium molybdate (Na_2MoO_4) (99.5% purity, Sigma-Aldrich) solution was introduced into the system at a drop rate of 0.2 mL/min. Then, the mixture was further ultrasonicated for 30 min to accelerate precipitation. The preformed white solution was transferred into a 40-mL teflon-lined stainless steel autoclave, which was sealed and placed into an electronic oven without shaking or stirring. The hydrothermal processing was performed at different temperatures (80–160 °C) and time (4–6 h). After hydrothermal treatment, the autoclave was allowed to cool to room temperature. The resulting solution was successively washed several times with distilled water and absolute ethanol. Finally, the white precipitates were collected and preserved in absolute ethanol for subsequent characterizations.

$PbMoO_4$ bulk crystals were obtained by directly mixing and continuously stirring isovolumetric solutions of 0.4 mol/L $PbCl_2$ and Na_2MoO_4. The resulting precipitate was then washed according to the aforementioned procedure and preserved in absolute ethanol.

The XRD patterns of the $PbMoO_4$ products were obtained using a Rigaku D/max 2550 X-ray diffractometer with CuKα radiation (λ = 0.15418 nm). FESEM experiments were performed on a field-emission scanning electron microscope (FEI Quanta 200F, Holland) at an acceleration voltage of 20 kV. The FTIR spectra of KBr powder-pressed pellets were recorded using a FTIR spectrometer (Nicolet NEXUS870, USA). PL and UV–VIS spectra were recorded using a luminescence spectrophotometer (Perkin–Elmer LS-55, USA) and Aligent 8453 UV–VIS spectrophotometer, respectively.

The XRD patterns of $PbMoO_4$ bulk crystals and nanoplates synthesized at 160 °C for 4 h are shown in Fig. 1. The XRD spectra reveals that all diffraction peaks of $PbMoO_4$ nanoplates and corresponding bulk crystals could be indexed to the scheelite-type tetragonal structure (lattice constants: $a = b = 0.5433$ nm, $c = 1.202$ nm, and $\alpha = \beta = \gamma = 90°$) without secondary phases, which

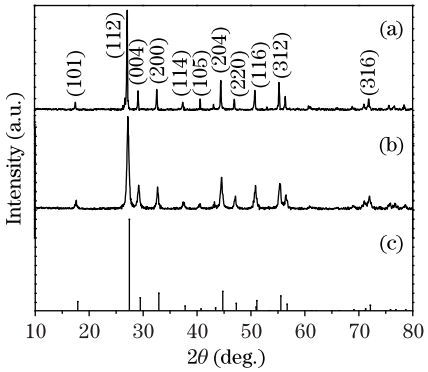

Fig. 1. XRD patterns of (a) $PbMoO_4$ bulk crystals, (b) nanoplates under condition of 80 °C for 6 h, and (c) JCPDS card (44-1486).

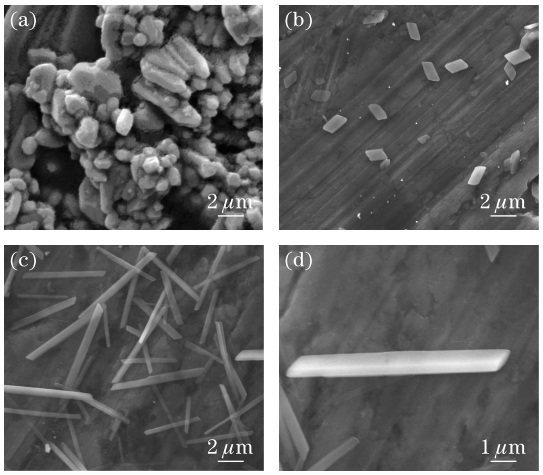

Fig. 2. FESEM images of (a) $PbMoO_4$ bulk crystals, (b) nanoplates synthesized at 80 °C for 6 h, (c) 160 °C for 4 h (× 15000 magnification), and (d) (× 30000 magnification), respectively.

concurs with the respective Joint Committee on Powder Diffraction Standards (JCPDS) card No. 44-1486[16] and the results[17]. The relative intensities and sharp diffraction peaks show that the $PbMoO_4$ were well crystallized. Additionally, broadening diffraction peaks were also observed among the $PbMoO_4$ nanoplates compared with corresponding bulk crystals, which should be attributed to the decrease in crystal size.

Figure 2 shows the FESEM micrographs of the $PbMoO_4$ bulk crystals and nanoplates produced using conventional hydrothermal combined with sonochemical method. $PbMoO_4$ bulk crystals obtained through conventional stirring are exceedingly irregular measuring several micrometers, as illustrated in Fig. 2(a). However, those processed via conventional hydrothermal and sonochemical method had regular plate-like shapes (Figs. 2(b)–(d)). In addition, different hydrothermal synthesis conditions produce correspondingly different surface morphologies and sizes. To describe their sizes accurately, a high magnification image of the $PbMoO_4$ nanoplates synthesized at 160 °C for 4 h are shown in Fig. 2(d) where the length of a $PbMoO_4$ nanoplate is ∼3 μm, and the corresponding width and height are ∼0.11 and ∼0.22 μm, respectively.

In this letter, FESEM micrographs were also employed to estimate the average particle size distribution of the $PbMoO_4$ nanoplates synthesized at 160 °C for 4 h. As shown in Fig. 3(a), the width distributions of $PbMoO_4$ nanoplates ranged from 0.15 to 0.30 μm. In addition, approximately 86% of the nanoplates have an average width ranging from 0.175 to 0.259 μm. Figure 3(b) shows the length distribution of the products ranging from 1.25 to 5.25 μm and approximately 83% have an average length ranging from 2.25 to 4.25 μm. These indicate that the $PbMoO_4$ nanoplates have a narrow particle size distribution.

Given its T_d-symmetry, the scheelite structure has four vibrations, specified as $\nu_1(A_1)$, $\nu_2(E)$, $\nu_3(F_2)$, and $\nu_4(F_2)$[19]. In lattice space, its spectrum is in accordance with the S_4 size symmetry.

Figure 4 illustrates the transmittance FTIR spectra of $PbMoO_4$ bulk crystals and nanoplates synthesized at 160 °C for 4 h. In Fig. 4(a), only the strong transmittance mode of the $PbMoO_4$ bulk crystal was observed at 720–900 cm^{-1}, which can be specified as the Mo-O anti-symmetric stretching vibration (ν_3) of the $[MoO_4]^{2-}$ tetrahedrons[19]. Additionally, a weak peak of the Mo-O bending mode (ν_4) is at 403 cm^{-1}, which is in good agreement with those previously reported[20]. As for the $PbMoO_4$ nanoplates, their transmittance vibration modes were in accordance with those of the molybdate compounds (Fig. 4(b)).

The PL emission process of molybdates is still not completely understood; consequently, several valid hypotheses were introduced in the literature to explain the origin of this physical property. For instance, Wu *et al.* argued that the $^1T_2 \rightarrow {}^1A_1$ electronic transitions within the $[MoO_4^{2-}]$ tetrahedron groups were responsible for the blue PL emission in the molybdates[21]. In contrast, Yang

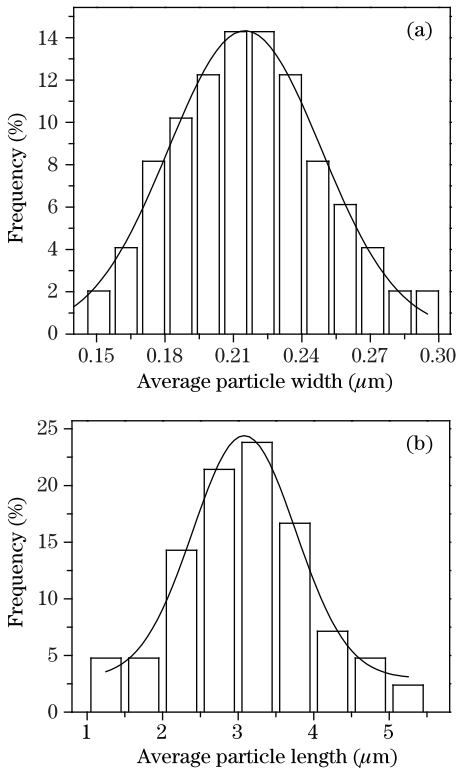

Fig. 3. (a) Average particle width and (b) length distributions of $PbMoO_4$ nanoplates synthesized at 160 °C for 4 h.

et al. attributed the origin of the PL properties to morphology, degree of crystallinity, and particle size[22].

Figure 5 presents the room-temperature PL spectra of the $PbMoO_4$ bulk crystals and nanoplates synthesized at 160 °C for 4 h. The PL spectra visibly illustrate broad bands from 320 to 520 nm. When excited at 250 nm, the $PbMoO_4$ bulk crystals exhibit a blue emission peak at 415 nm whereas the emission band of the $PbMoO_4$ nanoplates synthesized at 160 °C for 4 h blue-shifted at about 20 nm. Such a blue shift could be attributed to the decreased size, which concurs with the XRD results.

The equation proposed by Wood *et al*. is commonly used to estimate the optical band gap[23]. According to these authors, the optical band gap energy is related with absorbance and photon energy by equation as follows: $h\alpha\nu = (h\nu - E_{\rm gap})^n$, where α is the absorbance, h is the Planck constant, ν is the frequency, $E_{\rm gap}$ is the optical band gap, and n is a constant associated with the different types of electronic transitions. For the electronic transitions, n = 1/2, 2, 3/2, and 3 represent directed allowed, indirect allowed, direct forbidden, and indirect forbidden transitions, respectively. According to Lacomba-Perales *et al*., the molybdates and tungstates that had a scheelite-type tetragonal structure presented a direct allowed electronic transition[24]. Thus, the n=1/2 value was adopted as the standard.

In this letter, the $E_{\rm gap}$ values of the $PbMoO_4$ nanoplates and corresponding crystals were determined through extrapolation of the linear portion of the curve or tail, which is dependent on the degree of structural order-disorder level in the lattice and some other aspects,

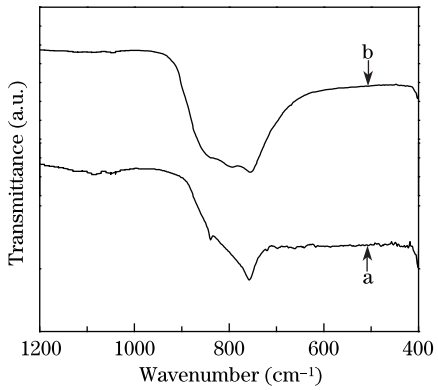

Fig. 4. FTIR spectra of $PbMoO_4$ bulk crystals (curve a) and nanoplates synthesized at 160 °C for 4 h (curve b).

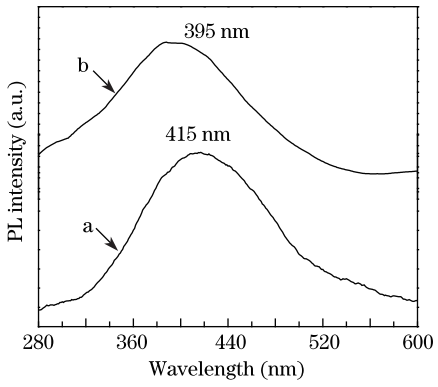

Fig. 5. PL spectra of $PbMoO_4$ bulk crystals (curve a) and nanoplates synthesized at 160°C for 4 h (curve b).

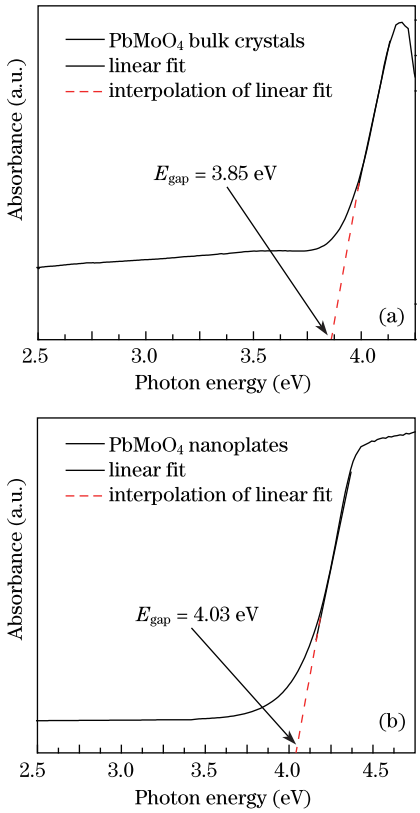

Fig. 6. UV-VIS absorption spectra of (a) $PbMoO_4$ bulk crystals and (b) nanoplates synthesized at 160 °C for 4 h.

including preparation method, shape, and experimental conditions[17]. The UV–VIS absorption spectra of the as-prepared $PbMoO_4$ bulk crystal and nanoplates synthesized at 160 °C for 4 h are shown in Fig. 6. The optical band gap of the nanoplates (4.03 eV) is wider than that of the bulk crystal material (3.85 eV). These results concur with the previously reported data in Ref. [25], indicating a possible transfer from the intermediate level to the optical band gap (valence band and conduction band), caused by the decrease in crystal size. This further verifies the XRD and PL results.

In conclusion, $PbMoO_4$ nanoplates that have excellent optical properties were synthesized through conventional hydrothermal with sonochemical method. Both the XRD and FTIR results have confirmed the similarity of the crystalline structures to that of the bulk material. Moreover, their optical properties, such as PL and UV–VIS, are clearly dependent on the crystal size.

This work was supported by the Shanghai Municipality Natural Science Foundation (No. 09ZR1431200), the Shanghai Municipality Education Committee Foundation (Nos. 10YZ182 and 09ZZ196), and the Shanghai Leading Academic Discipline Project (No. J51504).

References

1. X. Wu, C. Zou, W. Wei, F. Sun, G. Guo, and Z. Han, Chin. Opt. Lett. **8,** 709 (2010).
2. Q. Wei, Z. Ren, Z. He, and Z. Niu, Chin. Opt. Lett. **7,** 52 (2009).
3. X. Y. He, R. P. Jia, C. F. Ouyang, X. Wang, and J. H. Yang, Nano: Brife Reports and Reviews **2,** 383 (2007).

4. J. C. Sancoski, L. S. Cavalcante, M. R. Joya, J. A.Varela, P. S. Pizani, and E. Longo, Chem. Eng. J. **140,** 632 (2008).
5. L. S. Cavalcante, J. C. Sczancoski, V. C. Albarici, J. M. E. Matos, J. A. Varela, and E. Longo, Mater. Sci. Eng. B **150,** 18 (2008).
6. M. Minowa, K. Itakura, S. Moriyama, and W. Ootani, Nuclear Instruments and Methods in Physics Research Section A **320,** 500 (1992).
7. A. Phuruangrat, T. Thongtem, and S. Thongtem, J. Phys. Chem. Solids **70,** 955 (2009).
8. I. Bavykina, G. Angloher, D. Hauff, M. Kiefer, F. Petricca, and F. Pröbst, Opt. Mater. **31,** 1382 (2009).
9. V. B. Mikhailik, H. Kraus, D. Wahl, H. Ehrenberg, and M. S. Mykhaylyk, Nuclear Instruments and Methods in Physics Research Section A **562,** 513 (2006).
10. Z. Li, J. Du, J. Zhang, T. Mu, Y. Gao, B. Han, and J. Chen, Mater. Lett. **59,** 64 (2005).
11. D. A. Spassky, S. N. Ivanov, V. N. Kolobanov, V. V. Mikhailin, V. N. Zemskov, B. I. Zadneprovski, and L. I. Potkin, Radiat. Meas. **38,** 607 (2004).
12. T. Thongtema, A. Phuruangrat, and S. Thongtem, J. Ceram. Process. Res. **9,** 189 (2008).
13. L. S. Cavalcante, J. C. Sczancoski, R. L. Tranquilin, M. R. Joya, P. S. Pizani, J. A.Varela, and E. Longo, J. Phys. Chem. Solids **69,** 2674 (2008).
14. P. Yang, G. Q. Yao, and J. H. Lin, Inorg. Chem. Commun. **7,** 389 (2004).
15. J. H. Ryu, B. G. Choi, J. W. Yoon, K. B. Shim, K. Machi, and K. Hamada, J. Lumin. **124,** 67 (2007).
16. Committee on Powder Diffraction Standard, "Powder diffraction File JCPDS Int. Centre Diffraction Data", PA 19073-3273, USA (2001).
17. J. C. Sczancoski, M. D. R. Bomio, L. S. Cavalcante, M. R. Joya, P. S. Pizani, J. A. Varela, E. Longo, M. S. Li, and J. A. Andrés, J. Phys. Chem. C **113,** 5812 (2009).
18. G. M. Clark and W. P. Doyle, Spectrochimica Acta **22,** 1441 (1966).
19. Z. C. Ling, H. R. Xia, D. R. Ran, F. Q. Liu, S. Q. Sun, J. D. Fan, H. J. Zhang, J. Y. Wang, and L. L. Yu, Chem. Phys. Lett. **426,** 85 (2006).
20. J. A. Gadsden, *IR Spectra of Minerals and Related Inorganic Compounds* (Butterworths, London,1975).
21. X. Wu, J. Du, H. Li, M. Zhang, B. Xi, H. Fan, Y. Zhu, and Y. Qian, J. Solid State Chem. **180,** 3288 (2007).
22. J. Yang, C. Lu, H. Su, J. Ma, H. Cheng, and L. Qi, Nanotechnology **19,** 035608 (2008).
23. D. L. Wood and J. Tauc, Phys. Rev. B **5,** 3144 (1972).
24. R. Lacomba-Perales, J. Ruiz-Fuertes, D. Errandonea, D. Martinez-Garcfa, and A. Segura, Eur. Phys. Lett. **83,** 37002 (2008).
25. R. M. Hazen, L. W. Finger, and J. W. E. Mariathasan, J. Phys. Chem. Solids **46,** 253 (1985).